Applied Materials Today 1 (2015) 45–51

Contents lists available at ScienceDirect

Applied Materials Today

journal homepage: www.elsevier.com/locate/apmt

Highly efficient PLEDs based on poly(9,9-dioctylfluorene) and Super Yellow blend with Cs_2CO_3 modified cathode

M.U. Hassan[a,b,*,1], Yee-Chen Liu[a,1], Kamran ul Hasan[c,d], H. Butt[e], Jui-Fen Chang[f], R.H. Friend[a]

[a] Cavendish Laboratory, University of Cambridge, JJ Thomson Avenue, Cambridge CB3 0HE, United Kingdom
[b] COMSATS Institute Information Technology, Shehzad Town, Park Road, Islamabad 44000, Pakistan
[c] Centres of Excellence in Science & Applied Technologies (CESAT), Islamabad, Pakistan
[d] Department of Science and Technology, Campus Norrköping, Linköping University, Bredgatan 34, SE-601 74 Norrköping, Sweden
[e] Department of Engineering, University of Cambridge, JJ Thomson Avenue, Cambridge CB3 0HE, United Kingdom
[f] Department of Optics and Photonics, National Central University, Chung-Li 32001, Taiwan

ARTICLE INFO

Article history:
Received 19 June 2015
Received in revised form 21 August 2015
Accepted 21 August 2015

Keywords:
Polyfluorenes
Poly(*para*-phenylenevinylenes)
Light emitting diodes
Interfacial engineering
Cathode modification

ABSTRACT

Polymer light emitting diodes (PLEDs) based on the blend of 90% poly(9,9-dioctylfluorene) (F8) and 10% Super Yellow (SY) were used as the emissive layer and it exhibited high luminous efficiency up to ~27 cd A^{-1}. Hole-trapping nature native to the proposed blend system and efficient electron injection via Al/Ca/Cs_2CO_3 cathode was used against the conventional ITO/PEDOT:PSS anode which provided a well-balanced charge transport across the emissive layer. Thereby, the scheme maximizes the radiative recombination of these excitons within the bulk and away from the cathode. Consequently, non-radiative quenching effects at the cathode surface were avoided which resulted in ultrahigh efficiency of such devices.

1. Introduction

There has been considerable interest in interfacial engineering of polymer light emitting diodes (PLEDs) in order to achieve perfect charge balance within the emissive layer and maximize the light output [1–3]. For this, different avenues have been explored including tuning the charge injection by introducing a hole transport layer at the anode surface [4,5], and use of an electron injection interlayer between the emissive layer and the cathode [6,7]. Emissive layers have also been tailored: this include using blends of polymers as emissive layer which offers the potential of energy transfer between the blended polymers and results in enhanced light output [8,9]. Multilayer light emitting diodes have also been realized [10,11]. Structural modifications in PLEDs have also been proposed to enhance the efficiency [12]. There are encouraging success stories for these methods and further research is being carried out not only to improve the performance of these devices, but also to meet the stringent requirements of specialized applications [13].

In the field of polymer light emitting devices, there has always been a quest to realize a system that combines all basic physical properties needed for high performance devices – efficient charge injection, their balanced transport within the emissive layer, high radiative recombination rate and excellent light outcoupling [3,7,12]. Many times, a trade-off is noticed between electrical and optical properties. The value for maximum possible current density is generally considered to be around 10 A cm^{-2} under DC operation [14]. However, PLEDs with ultrahigh efficiency show a much lower current density [15,16], and vice versa [17]. Optimization of the transport properties via tuning the electron and hole injections gives a maximum current density of ~2 A cm^{-2} in F8 based PLEDs, but luminous efficiency of this system is low [17]. Oyamada et al. achieved high current densities in organic light emitting diodes by using Cs-doped phenyldipyrenylphosphine oxide layer as electron injection layer, but the device had an external quantum efficiency of <1% [18]. Kabara et al. used thick devices and enhance the luminance efficiency of the PLEDs, but with low current density [16]. This has been explained as an effect of shifting of the emission zone away from the cathode that minimizes its non-radiative quenching and results in enhanced luminous efficiency. Whereas, the transport properties are worsened because of the large thickness of the emissive layer – thick devices are more prone to resistive heating. Ohmic contacts have also been exploited in order to enhance the current injection as well as the efficiency of these devices [19,20].

Here, we describe PLEDs which offer ultrahigh luminous efficiency, low operating voltage and reasonably large current density. We used two strategies in order to achieve these goals. Firstly,

* Corresponding author at: COMSATS Institute Information Technology, Shehzad Town, Park Road, Islamabad 44000, Pakistan.
E-mail address: muhammad_umair@comsats.edu.pk (M.U. Hassan).
[1] These authors contributed equally to this work.

http://dx.doi.org/10.1016/j.apmt.2015.08.005
2352-9407/

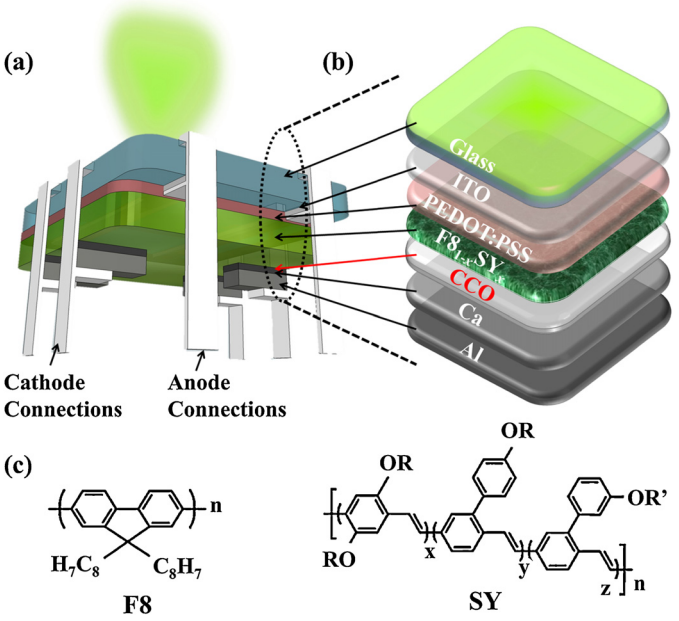

Fig. 1. (a) Schematic diagram of $F8_{1-x}SY_x$ ($x = 0$, 0.1 and 1) based PLED pixels. (b) Different layers in PLEDs. CCO interlayer is used in order to enhance the charge injection in the blend emissive layer. (c) Chemical structure of F8 and SY molecules.

a new polymer–polymer blend system $F8_{1-x}SY_x$ (x signifies the weight ratio) obtained by mixing poly(9,9-dioctylfluorene) (F8) and a poly (*para*-phenylenevinylene) (PPV) copolymer, Super Yellow (SY) was used as emissive layer (only $x = 0.1$ will be discussed in this work: this particular ratio (9:1) was selected because of its best performance (~21 cd A^{-1}) in conventional PLEDs structure, i.e. without CCO interlayer. Systematic evolution of the device performance with increasing weight concentration using conventional structure is the subject of a separate report). Although, these two polymers have already been studied extensively [21–24], here we use their blend as an emissive layer in PLEDs. Mixing them allows us to manipulate the hole-mobility by exploiting the difference present between their respective molecular orbital levels. We also considered the strong overlap between the emission spectra of F8 and absorption spectra of SY – the key parameter for an efficient Förster Resonance energy transfer (FRET) mechanism [25]. Secondly, we modified the conventional Ca/Al cathode scheme by introducing a thin Cs_2CO_3 (CCO) interlayer between $F8_{1-x}SY_x$ emissive layer and this cathode. Electron injection function and n-type doping effect of this interlayer is well-known [17,26–28]. We also investigated the role of CCO interlayer in our devices. Our scheme offered a good charge balance and resulted in ultrahigh efficiency of $F8_{0.9}SY_{0.1}$ based PLEDs. Note that there are also other materials such as caesium fluoride, lithium fluoride (LiF) and calcium (2) acetylacetonate which could be used as efficient electron injection layers [7,29,30]. It will be interesting to see their behaviour with the proposed blend system.

In this work, we used three types of emissive layers, pure F8, $F8_{0.9}$:$SY_{0.1}$ (9:1 being the weight ratio) and pure SY, and two different cathode assemblies, Ca/Al and CCO/Ca/Al (see schematics in Fig. 1). A comparative studywas made, where the effects of Ca/Al and CCO/Ca/Al cathode materials on luminous efficiency of different emissive layers were investigated – $F8_{0.9}SY_{0.1}$ based PLEDs will be the main focus. The 9:1 composition is selected after the studying the systematic evolution of the luminous efficiency, and noticing that this composition shows the best results. It also exhibits efficient Förster resonance energy transfer (however, these are the subjects of a separate report). $F8_{0.9}SY_{01}$ based PLEDs exhibit luminous efficiency η of ~20 cd A^{-1} with Ca/Al cathode, which is already considerably larger than the pure SY devices, $\eta \approx 12.5$ cd A^{-1}. Considerable improvement was made via interfacial engineering and introducing a CCO interlayer between the emissive layer and the cathode. CCO lowered the electron injection barrier and significantly enhanced the performance of as-made PLEDs – thereby, luminous efficiency of ~27 cd A^{-1} was achieved in $F8_{0.9}SY_{0.1}$ based devices.

2. Results and discussion

2.1. Current–voltage–luminance properties polymer blend light emitting diodes

Fig. 2a shows J–V characteristics of pure F8, $F8_{0.9}SY_{0.1}$ and pure SY based PLEDs with Ca/Al and CCO/Ca/Al cathodes. It was observed that the CCO interlayer produced pronounced effects on all kinds of devices. For F8 PLED, this interlayer reduced the turn-on voltage (V_{on}) from ~3.1 to ~2.8 V, and slightly increased the current density from ~1.1×10^2 to 2.8×10^2 mA cm^{-2} (at 5 V). V_{on} (~2.9 V) for $F8_{0.9}SY_{0.1}$ almost remained unchanged for both cathode schemes. However, after turn-on, current density ramps up more rapidly in CCO incorporated PLED and reach its maximum, ~1.5×10^3 mA cm^{-2} (at 9.5 V), and reaches only ~3.2×10^2 mA cm^{-2} (at 9.5 V) in PLED without the interlayer. SY gave a different picture: CCO interlayer did not change the turn-on voltage (~1.9 V with both cathode schemes), however, current density was reduced by one order of magnitude, from ~1.5×10^3 to 2.5×10^2 mA cm^{-2} (at 9.5 V). The turn-on voltage for light output ($V_{L\text{-}on}$) shows a decrease when interlayer is used in F8 and $F8_{0.9}SY_{0.1}$ based PLEDs, from ~3.6 to 3.1 V and from ~3.4 to 3 V, respectively, see L–V characteristics in Fig. 2b. CCO also resulted in considerably increased luminance across the whole voltage sweep for these devices: the value increased from ~1.1×10^2 to 3.2×10^3 cd m^{-2} (at 5 V) for pure F8, and from ~2.5×10^4 to 2.4×10^5 cd m^{-2} (at 9.3 V) for $F8_{0.9}SY_{0.1}$ based PLEDs. Pure SY shows a contrasting picture again: $V_{L\text{-}on}$ increased from ~2.4 to 2.9 V with introduction of CCO interlayer, while luminance reduced to ~14 times smaller value compared to the devices without this interlayer – there was a drop from ~1.3×10^5 to 9.4×10^3 cd m^{-2} (at 9.5 V). It was also noticed that, the luminous efficiency η for pure F8 and $F8_{0.9}SY_{0.1}$ PLEDs with CCO interlayer superseded the values without it, whereas, the trend was reversed in the case of pure SY PLEDs, see η–V in Fig. 2c. Using CCO interlayer increased the luminous efficiency for pure F8 device from ~1.7 (at 3.8 V) to 2.6 cd A^{-1} (at 3.2 V). The most efficient PLEDs were obtained when $F8_{0.9}SY_{0.1}$ blend was used as emissive layer and CCO interlayer was used at cathode side - we achieved highly efficient PLEDS, $\eta \approx 27$ cd A^{-1} (at 4 V), ~1.4 times larger than that obtained in blend PLED using Ca/Al cathodes scheme, $\eta_{max} \approx 20$ cd A^{-1} (at 5 V). It was also observed that the later value was the second highest value, ~1.6 times larger than pure SY PLEDs. Luminous efficiency of pure SY PLED with interlayer could only reach up to ~8.1 cd A^{-1} (at 4.1 V), which showed a poorer performance than that without CCO interlayer, ~12.5 cd A^{-1} (at 4.7 V).

2.2. Possible mechanism for high efficiency

We believe that it is the enhanced charge balance that enhanced the efficiency of $F8_{0.9}SY_{0.1}$ based PLEDs. There were two major avenues by which this has been possible. Firstly, *i* the intrinsic hole trapping nature of the blend slows down the hole transport, and improves the balance between electron and hole transport. Secondly, CCO interlayer increased the electron injection from the cathode side – thereby serving the same purpose. Energy band diagram helps us understand the possible mechanism of enhanced

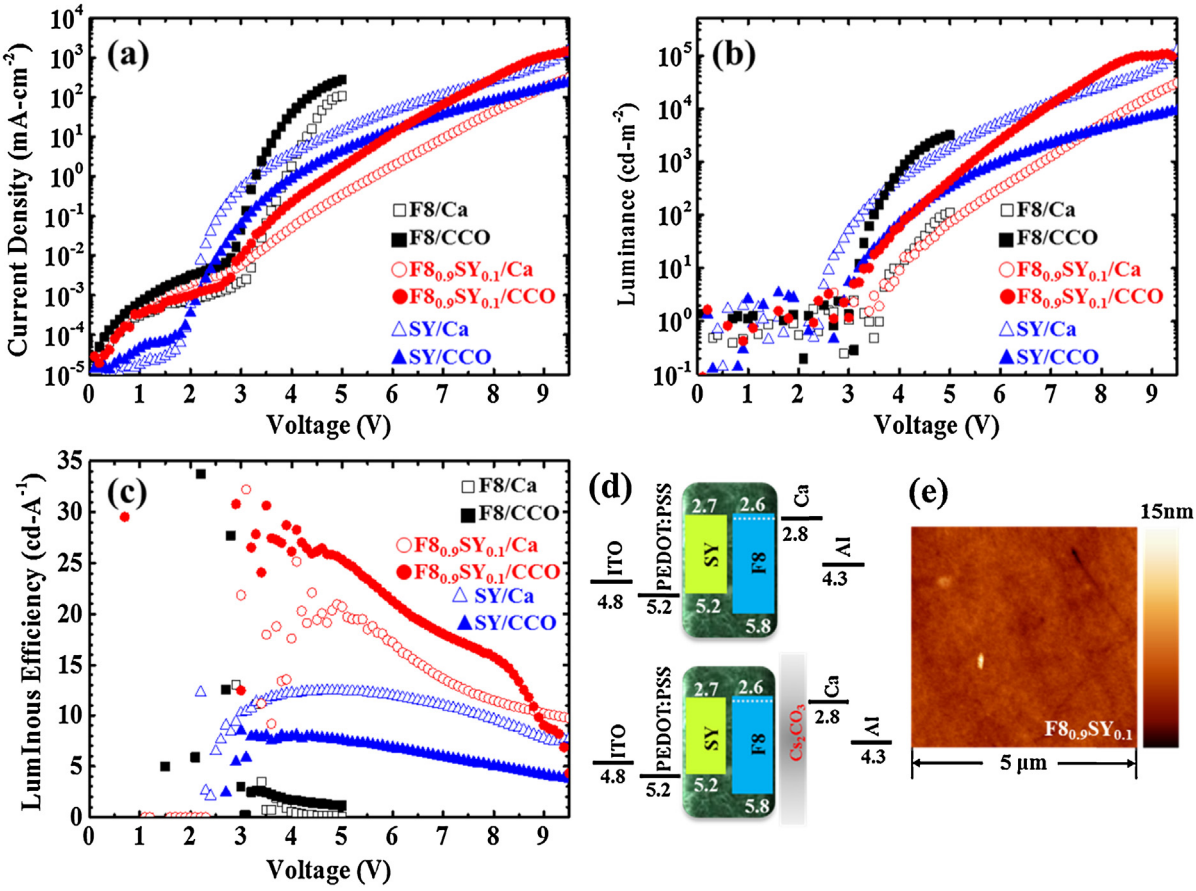

Fig. 2. Optoelectronic properties of pure F8, $F8_{0.9}SY_{0.1}$ and pure SY based PLEDs with (solid symbols) and without (open symbols) CCO interlayer: (a and b) Current density (/luminance) for F8 and $F8_{0.9}SY_{0.1}$ devices show increase with interlayer, but an opposite trend for SY devices across the whole voltage sweep, and (c) luminous efficiency shows the highest value, ~27cd A^{-1} for $F8_{0.9}SY_{0.1}$ PLED with CCO-interlayer and second highest for Ca/Al cathode. (d) Band diagrams for all kind of devices: blending F8 and SY results in the increased performance because of hole traps offered by SY molecules in the blend which introduces a balance between electron and hole transport. CCO interlayer enhances the electron injection and consequently raises the efficiency. White dash line in F8 depicts the β phase LUMO level ~2.7 eV. (e) AFM image of $F8_{0.9}SY_{0.1}$ shows a smooth surface without any noticeable phase separation/preferred structures.

efficiency, Fig. 2d: blue emitting F8 has a wider bandgap (~3.2 eV), as compared to SY (~2.5 eV) which gives off yellowish green emission [31,32]. Both polymers have their respective lowest occupied molecular orbital (LUMO) levels at ~2.7 eV. Therefore, we speculated that electron transport was negligibly hindered by the inclusion of small amount (10%) of SY in F8 (90%). However, the difference between HOMO levels of F8 (~5.8 eV) and SY (~5.2 eV) is considerably large (~0.6 eV). Due to this difference, mixing of SY molecules in F8 matrix results in the formation of strong hole trapping sites that severely hamper the hole current. Given that F8 and SY are both hole dominant polymers, i.e. hole mobility is larger than electron mobility in both pure systems [33–35]. However, hampered movement of holes in the blend offers a balance between electron and hole transport. Such balance, gives rise to the excitonic recombination within the bulk of the film, away from the cathode surface, suppressing the quenching of the radiative recombination at the cathode surface [36]. Subsequently, a columbic attraction between the opposite charge carriers improves the chances of radiative recombination of these excitons, resulting in enhanced efficiency for these PLEDs. The morphological details are also important and could contribute towards the device performance. However, we observed a smooth surface and no identifiable phase separation/preferred architectures in $F8_{0.1}SY_{0.9}$ films, see atomic force microscopic (AFM) image in Fig. 2e. Because of the enhanced electron injection from CCO/Ca/Al cathode, its incorporation into as-made PLEDs pushes the location of radiative recombination even further into the bulk of emissive layer, away from the cathode surface, and eventually augments the enhanced efficiency. It is important to note that FRET mechanism in blend LEDs has been extensively investigated and is considered a key parameter for enhanced efficiency [37]. However, this work shows that by modifying the transport via interfacial engineering at the electrode surfaces combined with clever tailoring of the active film can lead to significantly improved device performance. Here, efficient electron injection from cathode side and weakening of the hole dominant nature of the polymers were exploited successfully to achieve the desired results.

The luminous efficiency of the F8 PLED was improved because of increasing electron flux and hole blocking effect caused by the CCO interlayer, as confirmed by our single charge carrier devices (discussed later), consistent with Huang et al. [38]. However, the poor performance of SY based PLEDs could be because of the thickness of CCO interlayer (~2 nm), and this could be attributed to the narrowing of the emissive layer due to diffusion of CCO in pure SY. Although this interlayer enhances the electron injection, its n-type doping effect potentially quenches the excitonic emission via exciton–dopant and exciton–polaron quenching mechanism [39]. Suhonen et al. optimized the CCO thickness to 0.15 nm for the maximum efficiency [40]. Nonetheless, this does not imply that 0.15 nm thickness of interlayer should also be a preferable thickness for F8 and $F8_{0.9}SY_{0.1}$ devices (and this optimization needs a separate investigation). We maintained the thickness of CCO interlayer at 2 nm across all kinds of devices in order to maintain the consistency. Its role is investigated with help of single charge carrier devices,

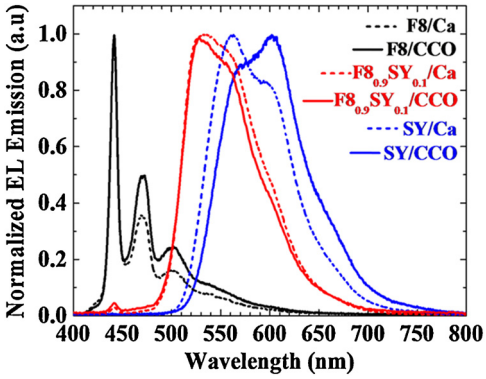

Fig. 3. Normalized EL spectra for F8, SY and $F8_{0.9}SY_{0.1}$ blend PLEDs with CCO interlayer (solid lines) compared with the devices that only have Ca/Al cathode (dashed lines) without interlayer. These EL spectra are shown for devices driven at 4 V.

which provides vital information about the interface behaviour of this interlayer.

2.3. Electroluminescent spectra

The EL spectra for F8, $F8_{0.9}SY_{0.1}$ and SY PLEDs with and without CCO showed interesting features, Fig. 3. In both cases, F8 PLEDs showed a peak at ~441 nm beside its main peak, which indicated a β-phase embedded in F8 amorphous phase matrix [41]. In addition, both F8 EL spectra (with and without CCO) have broad, featureless green emission located around 530 nm. This additional green emission is associated with on-chain defects incorporated during the synthesis [42,43]. Their oxidation leads to the presence of ketone defects and causes a trap behaviour for hole and electron transport [44]. In addition, this green emission may also be caused by interchain interaction [45]. The reason for the increasing long wavelength emission from CCO incorporated devices may come from the increasing amount of electrons being trapped in the F8 emitting layer before recombination. As more electrons transport in the lowest unoccupied molecular orbital (LUMO) level, there is an increased possibility of charges trapped at the lower energy sites. For $F8_{0.9}SY_{0.1}$ PLEDs, the EL spectra have slightly different shapes in both cases: devices without (with) CCO interlayer showed broad electronic 0–0 peak at 536 nm (530 nm) and first vibronic 0–1 peaks at 562 nm (562 nm), respectively. A slight narrowing of ~9 nm in full width half maximum was observed with the interlayer. It was also noticed that there was almost no signature from F8 (90%) with merely a small mixture of SY (10%) in the EL spectra for $F8_{0.9}SY_{0.1}$ based devices. However, peaks were strongly blue shifted compared with EL of pure SY PLED: the EL spectra for pure SY PLED without (with) CCO interlayer showed the electronic 0–0 peak at 561 nm (570 nm) and first vibronic peak 0–1 peak at 601 nm (606 nm), respectively, consistent with [46]. Emissions at longer wavelength in pure SY devices were attributed to the aggregate formation which resulted in interchange interactions at lower energies [47,48]. Whereas, this situation was diluted in farther spread SY molecules present in F8 host, resulting the emission to shift at higher energies.

The CIE (Commission Internationale de l'Eclairage) colour coordinates relative to the EL spectra shows clear colour change for (a) incorporation of CCO interlayer, and (b) incorporation of SY in F8: For pure F8 device the colour is deep blue which somewhat moves towards green and red sides with incorporation of CCO. There is almost no difference between the colours of $F8_{0.9}SY_{0.1}$ devices with both cathode configurations. However, for pure SY devices, incorporation of CCO considerably moves the colour towards red – resulting in orange colour. The snapshots have also been taken during operation of these PLEDs, see CIE colour coordinates and snapshots in Fig. 4.

2.4. Single charge carrier devices

Enhanced Electron Only Devices: In order to explain the role of CCO interlayer and charge transport mechanism, we fabricated enhanced electron only (EEODs) and hole blocking devices (HBDs) using pure and blended polymer ($F8_{1-x}SY_x$, where x is 0 or 1 for pure and 0.1 for the blend for convenience).

The schematics of EEODs (glass/ITO/ZnO/CCO/$F8_{1-x}SY_x$/CCO/Ca/Al) and its relative band diagram are shown in Fig. 5a. Reference devices (glass/ITO/ZnO/CCO/$F8_{1-x}SY_x$/Ca/Al) with no CCO interlayer were also made, and can be conceived by removing the interlayer in above figure. ZnO is commonly used as electron injection layer such as in inverted PLEDs, energy levels are according to Lee et al. [49]. Since CCO also works as electron injection layer, we use it on both sides of the polymer layer in EEODs [27].

From the *J–V* curves of both kinds of devices we can immediately appreciate that CCO interlayer caused dramatic effects on electron injection, Fig. 5b. Its incorporation increased the electronic current density J_e of F8 based EEOD by an order of magnitude, from ~87 to 7.9×10^2 mA cm^{-2} (at 5 V), consistent with Lu et al. [19]. By the same token, the effect was even more prominent for $F8_{0.9}SY_{0.1}$ based EEOD – J_e (~1.2×10^2 mA cm^{-2} at 3.9 V) and it exhibited 2 orders of magnitude larger than the device with Ca/Al cathode scheme. J_e (~38 mA cm^{-2} at 3.9 V) was also observed to be larger in SY based electron only devices with CCO, compared to 0.4 mA cm^{-2} without this interlayer. These experimental findings suggest that CCO interlayer increases the electronic flux within the emissive layer – it is one of the reasons which dictate higher efficiency of PLEDs having this interlayer. This large increase in electron current density in devices with SY content using CCO interlayer at cathode interface is a known feature of PFOs and PPV derivatives [49].

Hole Blocking Devices: After the confirmation of J_e enhancement behaviour of CCO, we investigated if the interlayer can also perform a hole blocking function. In order to probe this, HBDs (Glass/ITO/PEDOT:PSS/$F8_{1-x}SY$/CCO/MoO_3/Au) and reference hole only devices (HODs) (Glass/ITO/PEDOT:PSS/$F8_{1-x}SY$/MoO_3/Au) were fabricated. The schematics of these devices and their relative energy band diagram can be conceived from Fig. 6a and b. MoO_3 has a deep work function (6.7 eV), and provides ohmic contact with polymers having deep HOMO levels such as F8 and poly(9,9-dioctylfluorene-alt-benzothiadiazole) (F8BT) [49,50] – its holes injection properties are well-established. Au layer on top of MoO_3 serves as electrical connection as well as protective capping layer. The work function of Au is taken from Lee et al. [49]. In HBDs, the behaviour of CCO interlayer was observed to be different for each emissive layers. A comparison of *J–V* characteristics of F8, $F8_{0.9}SY_{0.1}$ and SY based HBDs with and without CCO interlayer with positive biasing from the MoO_3 side is given in Fig. 6c. The hole blocking effect is clearly observed in the F8 (SY) devices devices – J_h is suppressed by 7 (2) orders of magnitude with the introduction of CCO interlayer. The value dropped from ~5×10^3 (~15) to 5.6×10^{-4} mA cm^{-2} (0.2 mA cm^{-2}) at 6 V. In contrast, hole blocking function of CCO interlayer for $F8_{0.9}SY_{0.1}$ based devices could not be established – *J–V* curves almost retrace each other in both cases.

In order to double-check the hole blocking properties, these devices were also positively biased from the PEDOT:PSS side, Fig. 6d. In comparison with reference HBDs, CCO reduced the J_h from ~9 (~9.8×10^2) mA cm^{-2} to 5 (2) mA cm^{-2} at 6 V, in pure F8 (SY) HBDs. Interestingly, $F8_{0.9}SY_{0.1}$ devices with CCO showed an increase in hole current density: J_h increased from ~2.5 to ~1.3×10^3 mA cm^{-2} (at 6 V), compared to the devices without the CCO interlayer.

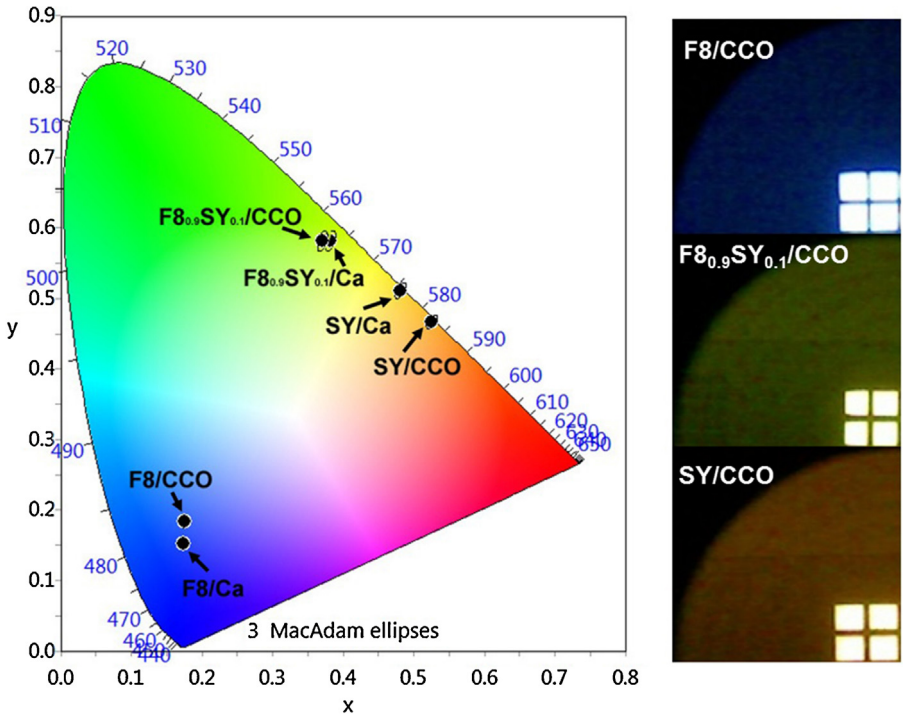

Fig. 4. The CIE colour coordinates relative to the EL spectra (left) and photograph of three corresponding devices with pure F8, $F8_{0.95}SY_{0.05}$ and pure SY emissive layers and CCO and interlayer (right). F8 devices emit in deep blue region which changes to yellowish green upon mixing of 10% of SY in F8. Pure SY device with CCO interlayer lies between green and red, giving off an orange effect.

Efficient Electron injection and hole blocking of Cs_2CO_3 are well established [51]. For pure devices, our results were consistent with the literature. However, behaviour of single charge carrier devices suggest that CCO interlayer enhances the electron injection in $F8_{0.9}SY_{0.1}$ based devices, but does not perform the hole blocking function. This behaviour was consistent in repeated experiments. We emphasize that understanding the exact nature of the interface between CCO and polymer is important in order to make a clear note on the observed behaviour of charge transport across $F8_{0.9}SY_{0.1}$/CCO interface.

We suggest that considerable improvement in efficiency can be made by optimizing the thickness of the $F8_{0.9}SY_{0.1}$ emissive layer and CCO interlayer. This has been proven very useful in other polymer systems [20,32].

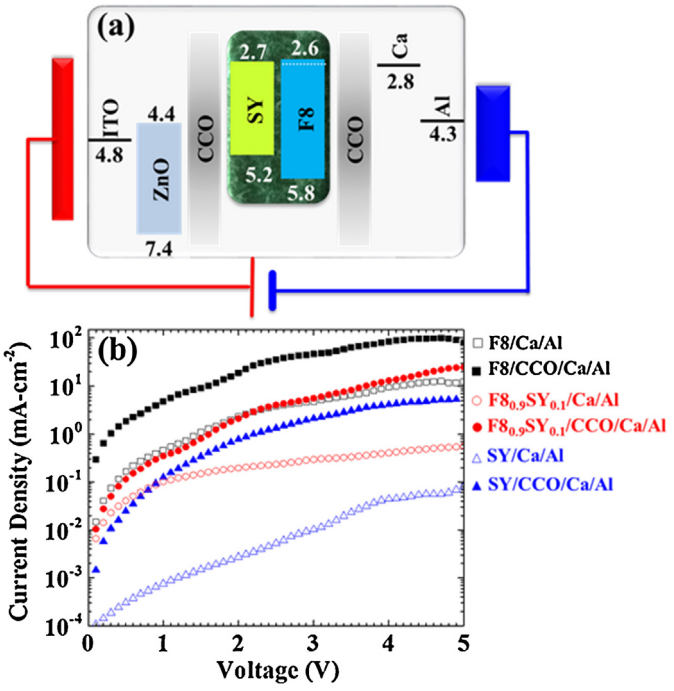

Fig. 5. (a) Energy band diagram (levels given in eV) of each layer in the enhanced electron only devices (glass/ITO/ZnO/CCO/$F8_{1-x}SY_x$/CCO/Ca/Al) and their operation mode. In the reference devices (glass/ITO/ZnO/CCO/$F8_{1-x}SY_x$/CCO/Ca/Al), CCO is not used between the polymer blend and Ca/Al cathode. (b) *J–V* curves of electron only devices with and without CCO interlayer at cathode, shown by solid and open symbols, respectively. All three kinds of devices exhibit increase in the current density as a result of enhanced electron injection from CCO/Ca/Al side.

3. Summary

In summary we have presented $F8_{0.9}SY_{0.1}$ based PLEDs, which showed ultrahigh efficiency up to ~27 cd A^{-1}. This excellent performance was because of intrinsic hole trapping nature of the blend system, which was further enhanced by accomplishing a perfect charge balance via efficient electron injection. The difference (~0.6 eV) between the HOMO levels of F8 (~5.8 eV) and SY (~5.2 eV) facilitated the formation of hole traps within the blend, resulting in significant reduction of hole transport. Because SY is present only in a small amount (10%) F8 matrix, and LUMOs of both polymers are almost at the same level (~2.7 eV), the electron transport is dominated by F8 molecules – therefore, remains unchanged. Thus, a balance between the charges was created, which dictated most of the exciton formation and recombination within the bulk of the film (away from the cathode surface). This charge balance was further enhanced by increasing the electron injection via Cs_2CO_3 interlayer between Ca/Al cathode and the emissive layer. Consequently, combined effect of the hole traps offered by SY molecules and enhancement of electron injection by interface engineering resulted into ultrahigh performance of $F8_{0.9}SY_{0.1}$ based PLEDs.

4. Experimental

Fabrication: (*Note*: each layer was synthesized under thesame condition for uniformity in all fabricated devices.) Indium-tin-oxide

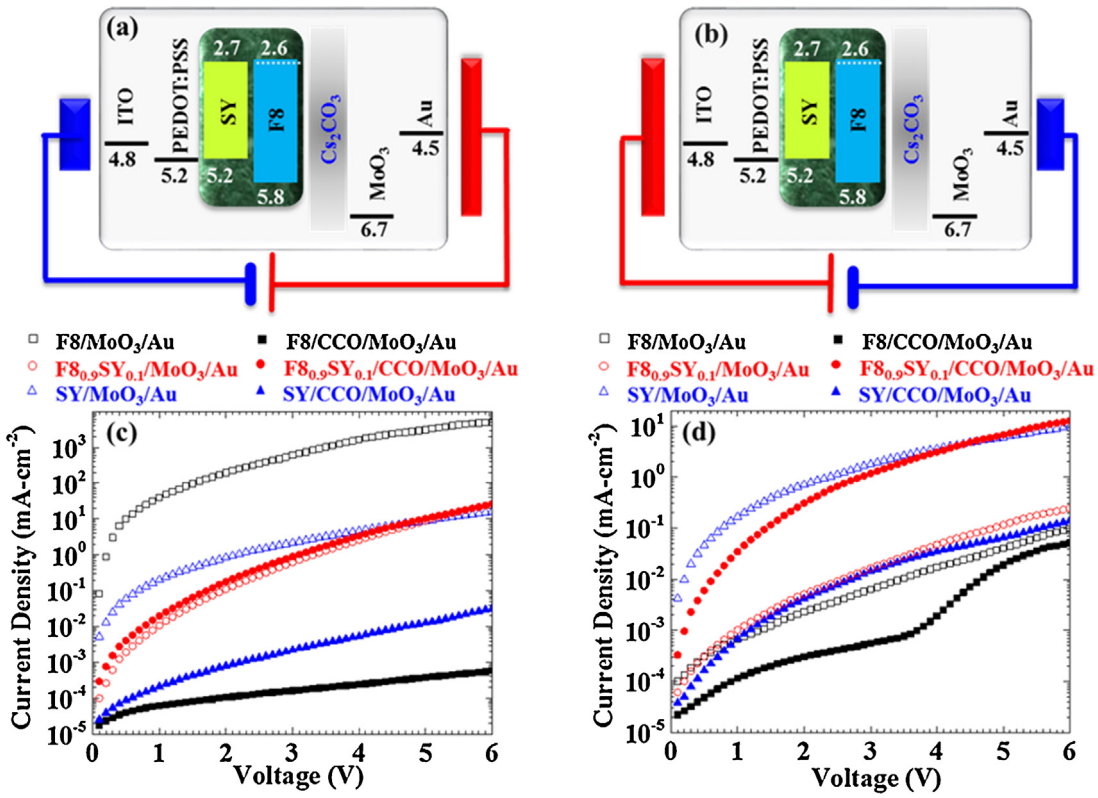

Fig. 6. (a and b) Energy band diagram of each layer in the hole only devices (glass/ITO/PEDOT:PSS/$F8_{1-x}SY_x$/CCO/MoO_3/Au) and their two operation modes (positively and negatively biased from MoO_3/Au side, respectively). In the reference device (glass/ITO/PEDOT:PSS/$F8_{1-x}SY_x$/MoO_3/Au), CCO layer is not used between the polymer blend and MoO_3/Au electrode. (c and d) *J–V* curves for hole only devices, positively biased from MoO_3 and PEDOT:PSS side, respectively: Both polarities show hole blocking effect for F8 and SY devices when CCO interlayer is used – current density is lesser as compared with the devices without this interlayer. There is almost no change in the current density for $F8_{0.9}SY_{0.1}$ based devices when positively bias from MoO_3, and there is increase for the opposite polarity – CCO does not act as a hole blocking layer for as-made devices.

(ITO) substrates were cleaned in an ultrasonic bath using acetone and isopropanol (10 min each). After cleaning, these substrates were treated with oxygen plasma. This was followed by spin-coating of PEDOT:PSS (50 nm) and then annealing under nitrogen environment at 230 °C for 30 min. Blend of F8 (294 kg mol^{-1}, Cambridge Display Technology,) and SY (Merk, 616 kg mol^{-1}) in chlorobenzene was prepared and spin-coated to obtain $F8_{1-x}SY_x$ films. The thickness of these films was optimized to around 100 ± 10 nm, confirmed by Dektak profilometer (similar films were also coated on quartz substrates for optical measurements). After the deposition of active layer, the devices were annealed at 70 °C for 30 min in nitrogen. Electron injection layer comprised of Ca/Al (3 nm/300 nm) was thermally deposited in a vacuum chamber incorporated inside a nitrogen glovebox. Cs_2CO_3 (Sigma Alrich) was dissolved in 2-methoxyethanol (5 g L^{-1}, Fluka) and spin-coated on ZnO layer. We obtained 2 nm thick Cs_2CO_3 layer by keeping spin-speed at 6000 rpm. After completing the fabrication of active part, electrical contacts were made using push-fit leadframes. Finally, the devices were encapsulated for stable air operation. For hole injection layer in hole only devices, MoO_3/Au (10 nm/70 nm) electrodes were made using thermal evaporation in the same chamber as described above for electron injection layer. For electron only devices, ZnO (50 nm) layer was deposited by spray pyrolysis on heated ITO substrates kept at 370 °C. Organic precursor zinc acetate dihydrate (Fluka) dissolved in anhydrous methanol (80 g L^{-1}) was used for this deposition.

Characterization: Current density–voltage–luminance (*J–V–L*) measurements of PLEDs were performed in ambient temperature using computer controlled sourcemeter (Keithley 2400) and chromameter (Minolta CS-200). Electroluminescence (EL) spectra were taken using Ocean Optics spectrometer (USB2000). For photoluminescence experiments, the polymer films were excited with 3–5 ns (10 Hz) laser pulses obtained from a compact housing of the nanosecond optical parametric oscillator (OPO) system and Nd:YAG Q-switched laser (NT342B, EDSPLA). The spectra were taken using 500 mm spectrograph, (SpectraPro2500i, Princeton Instruments) with incorporated CCD camera (Pix 100-F, Princeton Instruments).

Acknowledgements

Authors are thankful to Dr. Bodo and Dr. Sebastian Shriefer for their useful discussions.

References

[1] M. Kuik, G.J.A. Wetzelaer, H.T. Nicolai, N.I. Craciun, D.M. De Leeuw, P.W. Blom, 25th anniversary article: charge transport and recombination in polymer light-emitting diodes, Adv. Mater. 26 (2014) 512–531.
[2] R. Friend, R. Gymer, A. Holmes, J. Burroughes, R. Marks, C. Taliani, D. Bradley, D. Dos Santos, J. Bredas, M. Lögdlund, Electroluminescence in conjugated polymers, Nature 397 (1999) 121–128.
[3] P.K. Ho, J.-S. Kim, J.H. Burroughes, H. Becker, S.F. Li, T.M. Brown, F. Cacialli, R.H. Friend, Molecular-scale interface engineering for polymer light-emitting diodes, Nature 404 (2000) 481–484.
[4] T. Brown, J. Kim, R. Friend, F. Cacialli, R. Daik, W. Feast, Built-in field electroabsorption spectroscopy of polymer light-emitting diodes incorporating a doped poly (3,4-ethylene dioxythiophene) hole injection layer, Appl. Phys. Lett. 75 (1999) 1679–1681.
[5] J.S. Teguh, T.C. Sum, E.K. Yeow, Effect of charge accumulation on the stability of PEDOT: PSS during device operation, Chem. Phys. Lett. 607 (2014) 52–56.
[6] T. Brown, R. Friend, I. Millard, D. Lacey, T. Butler, J. Burroughes, F. Cacialli, Electronic line-up in light-emitting diodes with alkali-halide/metal cathodes, J. Appl. Phys. 93 (2003) 6159–6172.
[7] P. Piromreun, H. Oh, Y. Shen, G.G. Malliaras, J.C. Scott, P.J. Brock, Role of CsF on electron injection into a conjugated polymer, Appl. Phys. Lett. 77 (2000) 2403–2405.

[8] S. Tasch, E. List, O. Ekström, W. Graupner, G. Leising, P. Schlichting, U. Rohr, Y. Geerts, U. Scherf, K. Müllen, Efficient white light-emitting diodes realized with new processable blends of conjugated polymers, Appl. Phys. Lett. 71 (1997) 2883–2885.
[9] A. van Dijken, J.J. Bastiaansen, N.M. Kiggen, B.M. Langeveld, C. Rothe, A. Monkman, I. Bach, P. Stössel, K. Brunner, Carbazole compounds as host materials for triplet emitters in organic light-emitting diodes: polymer hosts for high-efficiency light-emitting diodes, J. Am. Chem. Soc. 126 (2004) 7718–7727.
[10] A. Brown, N. Greenham, J. Burroughes, D. Bradley, R. Friend, P. Burn, A. Kraft, A. Holmes, Electroluminescence from multilayer conjugated polymer devices: spatial control of exciton formation and emission, Chem. Phys. Lett. 200 (1992) 46–54.
[11] X. Gong, S. Wang, D. Moses, G.C. Bazan, A.J. Heeger, Multilayer polymer light-emitting diodes: white-light emission with high efficiency, Adv. Mater. 17 (2005) 2053–2058.
[12] T.W. Koh, J.M. Choi, S. Lee, S. Yoo, Optical outcoupling enhancement in organic light-emitting diodes: highly conductive polymer as a low-index layer on microstructured ITO electrodes, Adv. Mater. 22 (2010) 1849–1853.
[13] E.B. Namdas, M. Tong, P. Ledochowitsch, S.R. Mednick, J.D. Yuen, D. Moses, A.J. Heeger, Low thresholds in polymer lasers on conductive substrates by distributed feedback nanoimprinting: progress toward electrically pumped plastic lasers, Adv. Mater. 21 (2009) 799–802.
[14] T. Matsushima, H. Sasabe, C. Adachi, Carrier injection and transport characteristics of copper phthalocyanine thin films under low to extremely high current densities, Appl. Phys. Lett. 88 (2006), 033508-033508-3.
[15] N. Corcoran, A. Arias, J. Kim, J. MacKenzie, R. Friend, Increased efficiency in vertically segregated thin-film conjugated polymer blends for light-emitting diodes, Appl. Phys. Lett. 82 (2003) 299–301.
[16] D. Kabra, L.P. Lu, M.H. Song, H.J. Snaith, R.H. Friend, Efficient single-layer polymer light-emitting diodes, Adv. Mater. 22 (2010) 3194–3198.
[17] C.C. Hsiao, A.E. Hsiao, S.A. Chen, Design of hole blocking layer with electron transport channels for high performance polymer light-emitting diodes, Adv. Mater. 20 (2008) 1982–1988.
[18] T. Oyamada, H. Sasabe, C. Adachi, S. Murase, T. Tominaga, C. Maeda, Extremely low-voltage driving of organic light-emitting diodes with a Cs-doped phenyldipyrenylphosphine oxide layer as an electron-injection layer, Appl. Phys. Lett. 86 (2005), 033503-033503-3.
[19] L.P. Lu, D. Kabra, K. Johnson, R.H. Friend, Charge-carrier balance and color purity in polyfluorene polymer blends for blue light-emitting diodes, Adv. Funct. Mater. 22 (2012) 144–150.
[20] L.P. Lu, C.E. Finlayson, R.H. Friend, Thick polymer light-emitting diodes with very high power efficiency using Ohmic charge-injection layers, Semicond. Sci. Technol. 29 (2014), 025005.
[21] X. Gong, P.K. Iyer, D. Moses, G.C. Bazan, A.J. Heeger, S.S. Xiao, Stabilized blue emission from polyfluorene-based light-emitting diodes: elimination of fluorenone defects, Adv. Funct. Mater. 13 (2003) 325–330.
[22] I. Ghosh, A. Mukhopadhyay, A.L. Koner, S. Samanta, W.M. Nau, J.N. Moorthy, Excited-state properties of fluorenones: influence of substituents, solvent and macrocyclic encapsulation, Phys. Chem. Chem. Phys. 16 (2014) 16436–16445.
[23] E.B. Namdas, J.S. Swensen, P. Ledochowitsch, J.D. Yuen, D. Moses, A.J. Heeger, Gate-controlled light emitting diodes, Adv. Mater. 20 (2008) 1321–1324.
[24] N. Kaihovirta, A. Asadpoordarvish, A. Sandström, L. Edman, Doping-induced self-absorption in light-emitting electrochemical cells, ACS Photonics 1 (2014) 182–189.
[25] Y. Shirasaki, G.J. Supran, M.G. Bawendi, V. Bulović, Emergence of colloidal quantum-dot light-emitting technologies, Nat. Photonics 7 (2013) 13–23.
[26] G. Li, C.-W. Chu, V. Shrotriya, J. Huang, Y. Yang, Efficient inverted polymer solar cells, Appl. Phys. Lett. 88 (2006), 253503-253503-3.
[27] J. Huang, Z. Xu, Y. Yang, Low-work-function surface formed by solution-processed and thermally deposited nanoscale layers of cesium carbonate, Adv. Funct. Mater. 17 (2007) 1966–1973.
[28] Y. Vaynzof, D. Kabra, L.L. Chua, R.H. Friend, Improved electron injection in poly(9,9′-dioctylfluorene)-co-benzothiodiazole via cesium carbonate by means of coannealing, Appl. Phys. Lett. 98 (2011), 113306-113306-3.
[29] T. Hasegawa, S. Miura, T. Moriyama, T. Kimura, I. Takaya, Y. Osato, H. Mizutani, Novel electron-injection layers for top-emission OLEDs, in: SID Symposium Digest of Technical Papers, 2004, pp. 154–157.
[30] Q. Xu, J. Ouyang, Y. Yang, T. Ito, J. Kido, Ultrahigh efficiency green polymer light-emitting diodes by nanoscale interface modification, Appl. Phys. Lett. 83 (2003) 4695–4697.
[31] A.J. Campbell, D.D. Bradley, H. Antoniadis, Quantifying the efficiency of electrodes for positive carrier injection into poly(9,9-dioctylfluorene) and representative copolymers, J. Appl. Phys. 89 (2001) 3343–3351.
[32] H.J. Bolink, E. Coronado, J. Orozco, M. Sessolo, Efficient polymer light-emitting diode using air-stable metal oxides as electrodes, Adv. Mater. 21 (2009) 79–82.
[33] X. Zhang, Q. Hu, J. Lin, Z. Lei, X. Guo, L. Xie, W. Lai, W. Huang, Efficient and stable deep blue polymer light-emitting devices based on β-phase poly(9,9-dioctylfluorene), Appl. Phys. Lett. 103 (2013), 153301.
[34] E.B. Namdas, P. Ledochowitsch, J.D. Yuen, D. Moses, A.J. Heeger, High performance light emitting transistors, Appl. Phys. Lett. 92 (2008), 183304.
[35] P. Blom, M. De Jong, J. Vleggaar, Electron and hole transport in poly(p-phenylene vinylene) devices, Appl. Phys. Lett. 68 (1996) 3308–3310.
[36] A.L. Burin, M.A. Ratner, Exciton migration and cathode quenching in organic light emitting diodes, J. Phys. Chem. A 104 (2000) 4704–4710.
[37] B.R. Lee, W. Lee, T.L. Nguyen, J.S. Park, J.-S. Kim, J.Y. Kim, H.Y. Woo, M.H. Song, Highly efficient red-emitting hybrid polymer light-emitting diodes via Forster resonance energy transfer based on homogeneous polymer blends with the same polyfluorene backbone, ACS Appl. Mater. Interfaces 5 (2013) 5690–5695.
[38] J. Huang, G. Li, E. Wu, Q. Xu, Y. Yang, Achieving high-efficiency polymer white-light-emitting devices, Adv. Mater. 18 (2006) 114–117.
[39] C. Williams, S. Lee, J. Ferraris, A.A. Zakhidov, Exciton–dopant and exciton–charge interactions in electronically doped OLEDs, J. Lumin. 110 (2004) 396–406.
[40] R. Suhonen, R. Krause, F. Kozlowski, W. Sarfert, R. Pätzold, A. Winnacker, Performance and stability of poly(phenylene vinylene) based polymer light emitting diodes with caesium carbonate cathode, Org. Electron. 10 (2009) 280–288.
[41] B. Arredondo, B. Romero, A. Gutiérrez-Llorente, A. Martínez, A.L. Alvarez, X. Quintana, J.M. Otón, On the electrical degradation and green band formation in α-and β-phase poly(9,9-dioctyfluorene) polymer light-emitting diodes, Solid-State Electronics 61 (2011) 46–52.
[42] U. Scherf, E.J. List, Semiconducting polyfluorenes – towards reliable structure–property relationships, Adv. Mater. 14 (2002) 477–487.
[43] X. Gong, D. Moses, A.J. Heeger, S. Xiao, Excitation energy transfer from polyfluorene to fluorenone defects, Synth. Met. 141 (2004) 17–20.
[44] M. Sims, D.D. Bradley, M. Ariu, M. Koeberg, A. Asimakis, M. Grell, D.G. Lidzey, Understanding the origin of the 535 nm emission band in oxidized poly(9,9-dioctylfluorene): the essential role of inter-chain/inter-segment interactions, Adv. Funct. Mater. 14 (2004) 765–781.
[45] M. Kuik, G.J.A. Wetzelaer, J.G. Laddé, H.T. Nicolai, J. Wildeman, J. Sweelssen, P.W. Blom, The effect of ketone defects on the charge transport and charge recombination in polyfluorenes, Adv. Funct. Mater. 21 (2011) 4502–4509.
[46] E. Snedden, L. Cury, K. Bourdakos, A. Monkman, High photoluminescence quantum yield due to intramolecular energy transfer in the Super Yellow conjugated copolymer, Chem. Phys. Lett. 490 (2010) 76–79.
[47] U. Lemmer, S. Heun, R. Mahrt, U. Scherf, M. Hopmeier, U. Siegner, Aggregate fluorescence in conjugated polymers, Chem. Phys. Lett. 240 (1995) 373–378.
[48] T.-Q. Nguyen, V. Doan, B.J. Schwartz, Conjugated polymer aggregates in solution: control of interchain interactions, J. Chem. Phys. 110 (1999) 4068–4078.
[49] T.W. Lee, J. Hwang, S.Y. Min, Highly efficient hybrid inorganic–organic light-emitting diodes by using air-stable metal oxides and a thick emitting layer, ChemSusChem 3 (2010) 1021–1023.
[50] H. Nicolai, G. Wetzelaer, M. Kuik, A. Kronemeijer, B. de Boer, P. Blom, Space-charge-limited hole current in poly(9,9-dioctylfluorene) diodes, Appl. Phys. Lett. 96 (2010), 172107-172107-3.
[51] L. Jia-Rong, N. Fang-Fang, L. Ya-Wei, Z. Peng-Ju, Improved hole-blocking and electron injection using a TPBI Interlayer at the cathode interface of OLEDs, Chin. Phys. Lett. 28 (2011), 047803.